Letters

Active Thermal Control With Optimal Phase Angle Under Stall Condition of Machine Drive Inverter

Yuhao Qi, Ke Ma, *Senior Member, IEEE*, and Shihao Xia

***Abstract*—Active thermal control (ATC) is becoming a popular solution to improve the reliability of power semiconductor devices in electric machine drive systems. Conventional ATCs mostly focus on the extension of a lifetime under common mission profiles in relatively long-term timescale, but the ATCs under abnormal conditions, such as extreme overstress in relatively short-term timescale, still need further investigation. This letter proposes a novel ATC method by optimal phase angle to redistribute the electrothermal stress under the stall condition of the machine drive inverter. During the normal operation, the proposed method will not disturb the original drive control structure. During the stall condition, the maximum electrothermal stress in power semiconductor devices can be relieved significantly. With no extra fluctuating electromagnetic torque, mechanical stability can also be guaranteed. Simulations and experimental results are provided to validate the effectiveness of the proposed method.**

***Index Terms*—Active thermal control (ATC), electric machine drive, phase angle control, reliability, stall condition.**

I. Introduction

NOWADAYS, electric machine drive systems have been widely applied in various important fields, such as electric vehicles/transportations, aerospace, and high-precision industry procession. Compared with the electric machine which is mainly composed of electrothermal-durable materials, power electronics components in the drive system are much more fragile when suffering from severe electrothermal stress without any protection. As a result, enhancement for the reliability of power electronics semiconductor devices is becoming an emerging need [1]–[4].

In order to ease the electrothermal stress and improve the reliability of power electronics semiconductors, various active thermal control (ATC) are recently proposed for power electronics devices and converters [5]–[8]. For the application of electric machine drive, the electrothermal stress of power electronics can be classified into overstress in the short-term timescale (such as stall, rapid acceleration, and deceleration mission profile), and wear-out stress in the long-term timescale (such as constant or cycling mission profile).

According to the rain flow counting theory [9], most state-of-art ATCs focus on relieving the wear-out stress in a relatively long-term timescale via junction temperature limitation. However, in the application of electric machine drive systems whose fundamental frequency ranges widely, the consequence of the overstress in short-term timescale is of great importance. The overstress in power semiconductor devices will commonly occur under low-speed operation, especially the stall condition, under which the electric machine will be switched to the operation mode with dc load, resulting in significant rise and unbalanced distribution of junction temperature.

Several ATCs relieve the overstress under stall condition of electric machine are reported by manipulating the modulation signal, switching frequency, current level, and other control freedoms of power electronics converter. Ko *et al.* [10] and Karami *et al.* [11] proposed zero-speed modulation methods for power loss equalization in for two-level and three-level drive inverters. However, the zero-speed modulation methods will overconsume the calculation resources of controller, and the mode switching of converter may easily induce instability issues of the drive system. Wei *et al.* [115] proposed an ATC method to reduce the PWM frequency and switching losses, which can also be applied to the stall condition. However, the reduced switching frequency may significantly increase the current ripple, which in practice will induce fierce torque fluctuation and increased noise level.

In respect to the ATC for current stress limitation, Lemmens *et al.* [4] proposed an ATC to achieve redistribution between i_d and i_q in special field-weakening control method. However, this method is only suitable for the specific type of inner permanent synchronous motor. Ali *et al.* [13] proposed a current limiting and loss redistribution strategy. The current amplitude is repeatedly limited once the measured junction temperature exceeds the threshold. However, the immobility of the mechanical system cannot be guaranteed because the supporting electromagnetic torque is fluctuating, which may induce dangerous coasting of the electric vehicles on the slope.

In this letter, the optimal current stress distribution of power semiconductor devices under stall condition is analyzed. By introducing additional phase control loop, a novel ATC method with optimal phase angle (OPA) under stall condition of the machine drive system is proposed. The proposed method can redistribute and minimize the overall current stress in the three-phase of electric machine system, thus the junction temperature

Manuscript received February 6, 2022; revised March 9, 2022; accepted March 28, 2022. Date of publication April 20, 2022; date of current version May 23, 2022. This work was supported by the National Nature Science Foundation of China under Grant 51777123. *(Corresponding author: Ke Ma.)*

The authors are with the Key Laboratory of Control of Power Transmission and Conversion, Ministry of Education, Shanghai Jiao Tong University, Shanghai 200240, Chinaand also with the Department of Electrical Engineering, Shanghai Jiao Tong University, Shanghai 200240, China (e-mail: qiyuhao0@sjtu.edu.cn; kema@sjtu.edu.cn; xia0112@sjtu.edu.cn).

Color versions of one or more figures in this article are available at https://doi.org/10.1109/TPEL.2022.3164086.

Digital Object Identifier 10.1109/TPEL.2022.3164086

as well as power losses of power semiconductor devices can be redistributed and reduced significantly. The feasibility of the proposed method is validated by simulations and experiments.

Compared with the existing methods, superiorities of the proposed OPA control can be summarized as follows:

1) Through additional rotor position control, the maximum current stress can be limited to optimal, thereby indirectly realizing single-phase current zero. Compared with the method simply controlling single-phase current zero, the proposed OPA control method reserves the control behavior of the original current control loop, aiming at the rotor position, which is the top-level control freedom.
2) Considering asymmetry factors, such as thermal coupling effect, the maximum thermal stress can be flexibly adjusted through setting specific stall sector detection and rotor position reference. Correspondingly, current stress in specific phase can be controlled to zero flexibly, while the exiting ATC for current stress limitation can hardly realize.

II. Proposed Optimized Phase Angle Control Under Stall Condition

A. Analysis of Optimal Current Distribution

As key control freedom in ATC for electrothermal stress relief (such as modulation signal and switching frequency), the current level is focused in this letter. In order to relieve the current stress on the power semiconductor devices of the electric machine drive inverter under the stall condition, a reasonable stall electrical phase angle should also be designed, instead of controlling the current amplitude in the price of the stability of the mechanical system.

Instant maximum current stress on the power semiconductor devices of the drive inverter can significantly decide on the reliability of the target drive module in short-term timescale. Thus, the maximum current stress should be first limited. The maximum current stress is shown in Fig. 1(a), while the corresponding phase angles of stator current and rotor position are shown in Fig. 1(c). Within one fundamental cycle of the current, it can be found that the maximum current stress of power semiconductor devices reaches minimum at specific electrical phase angle $\mathrm{PA}_{\min}$, which can be expressed as

$$\begin{cases} \mathrm{PA}_{\min} = k \times \frac{\pi}{3} + \theta_{idq} \\ \text{where } k = 0, 1, 2, 3, 4, 5, 6 \; \theta_{idq} = \arctan \frac{i_d}{i_q} \end{cases} \tag{1}$$

where i_d and i_q are the stator current in dq axis, and θ_{idq} is the phase angle offset caused by stator current in d axis.

Second, in order to realize the optimal distribution, current stress should be redistributed among three phases according to the thermal characteristics of the drive converter. Minimum current stress should be distributed to the specific phase suffering the severest thermal coupling effect [14]. Fig. 1(b) shows the individual current stress on each phase, while Fig. 1(c) shows the corresponding electrical phase angle. Considering the minimum current stress on specific phases, $\mathrm{PA}_{\min}$ in (1) can be classified according to selected phase k, which can be expressed as

$$\begin{cases} \mathrm{PA}_{\text{mink}} = \theta_k + \theta_{idq} \text{ or } \theta_k + \theta_{idq} + \pi \\ \text{where } \theta_{k=A,B,C} = 0, \frac{2\pi}{3}, -\frac{2\pi}{3}; \theta_{idq} = \arctan \frac{i_d}{i_q} \end{cases} \tag{2}$$

where θ_k represents the variable phase angle const for the selected phase k.

In Fig. 1, k is selected as B phase because phase B is commonly connected to the middle position of the power semiconductor module, which always suffers the strongest thermal coupling effect. However, in other cases (modified power semiconductor devices electrical/physical arrangement), θ_k can be flexibly adapted for different conditions.

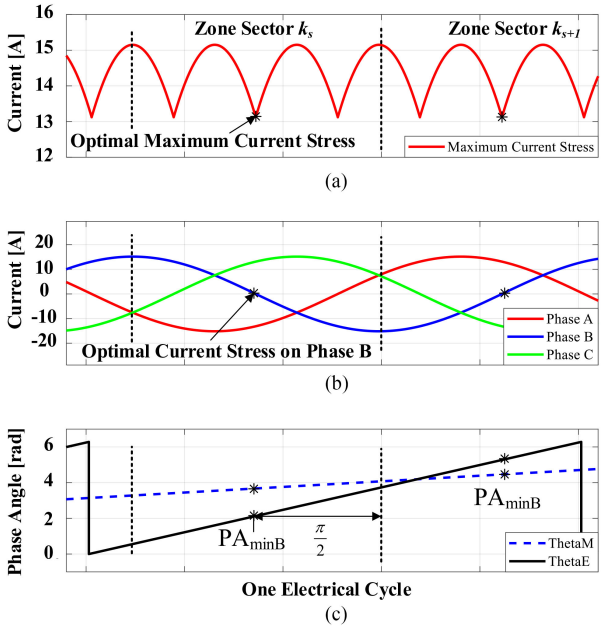

Fig. 1. Maximum and individual current stress with corresponding phase angle (dotted line: stall condition detection boundary, star point: optimal stall operation condition in case of phase B optimization). (a) Maximum current stress. (b) Individual current stress. (c) Electrical and mechanical phase angle.

Based on the limitation of stator maximum current stress and stator current redistribution, the reduction in power losses under the stall condition can be estimated according to the power losses model. For different types of power semiconductor devices, the ratio of reduction in power losses can varies from 13.4% $(1 - \frac{\sqrt{3}}{2})$ to 25% $(1 - (\frac{\sqrt{3}}{2})^2)$, compared with the worst situation. In other words, under the premise that the thermal paths of the system do not change, the ratio of the maximum temperature rise can vary from 13.4% to 25%.

B. Realization of Proposed OPA Control for Optimal Current Stress Distribution

According to the analysis above, the optimal current distribution can be realized by controlling specific electrical phase angles. Unfortunately, it is difficult to directly design a control system for electrical (current) phase angle based on the drive system (mechanical-control-based system). However, according to the model of electric machine [14], the electrical phase angle (current phase angle), and mechanical phase angle (rotor position phase angle) are linearly dependent under stall condition ($\omega_e = 0$), so that the control target can be simplified to the mechanical phase angle.

Fig. 2 shows the block diagram of the proposed mechanical OPA control system, based on the original drive control system, which is designed as follows:

First, the OPA reference of rotor position should be generated. To guarantee an acceptable mechanical/electrical phase angle shift, the OPA of stator current is separated into different stall zone sectors k_s (dotted line boundary). In each stall zone, there exists only one OPA θ_s (star point position), as shown in Fig. 1(c). The stall zone and OPA can be calculated by (3). The

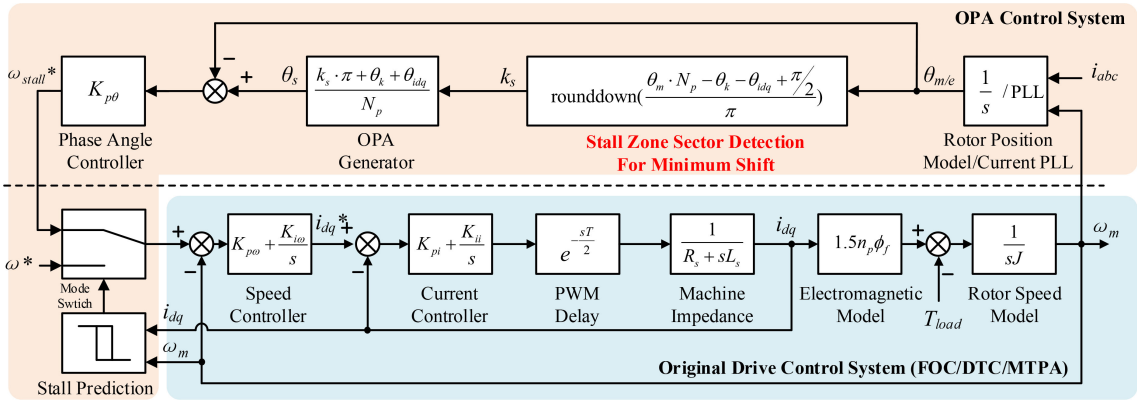

Fig. 2. Control diagram of the proposed OPA control and the original drive control system (FOC).

rotor position can be measured by highly precise encoder with current PLL assistant. Applying the stall sector zone separation, the maximum electrical phase angle shift can be limited to $\pi/2$

$$\begin{cases} k_s = \text{rounddown}\left(\frac{\theta_m \cdot N_p - \theta_k - \theta_{idq} + \pi/2}{\pi}\right) \\ \theta_s = \frac{k_s \cdot \pi + \theta_k + \theta_{idq}}{N_p} \\ \text{where } \theta_{k=A,B,C} = 0, \frac{2\pi}{3}, -\frac{2\pi}{3}, \theta_{idq} = \arctan\frac{i_d}{i_q}. \end{cases} \tag{3}$$

Second, the speed reference under the stall condition should be regenerated. The difference between the current mechanical phase angle and the generated optimal mechanical phase angle is calculated. Instead of the original speed reference, the speed reference under the stall condition will be generated through a proportional controller. When the OPA control system operates in a steady state, the maximum current stress is redistributed in the OPA.

Finally, the speed reference mode should be switched from the original signal to the generated one. In order to preswitch the control mode of the drive system, the coming stall condition must be predicted. The prediction can be realized through speed and electromagnetic torque detection (calculated by stator current), whose threshold should be designed according to the detailed operation capacity and device selection. What is more, the OPA control system is not applicable under certain specific situations, where the electric machine rotor is completely stuck by violent destruction instantaneously.

III. Simulation and Experimental Validations

To verify the feasibility of the proposed OPA control method and make a comparison with the original drive control system without OPA control, the simulations are carried out based on PLECS. The electric machine is controlled in field-oriented-control (FOC) mode. The power electronics module under test is chosen as STARPOWER GD50FFX65C5S. The parameters of the target PMSM are listed in Table II [116].

In the simulation, a mission profile is constructed, consisting of acceleration, deceleration, and stall condition, which is given as follows:

The rotational speed is set as 60 rpm at first in order to simulate the soft start of the target electric machine. At 2 s, the electric machine is accelerated to 1200 rpm within 3 s where the fundamental electrical frequency is 80 Hz. At 5 s, the rotor speed is decelerated to 0 rpm (stall condition) within 5 s. The load torque is set 2 N·m and steps to 3.5 N·m at 10 s. The comparison

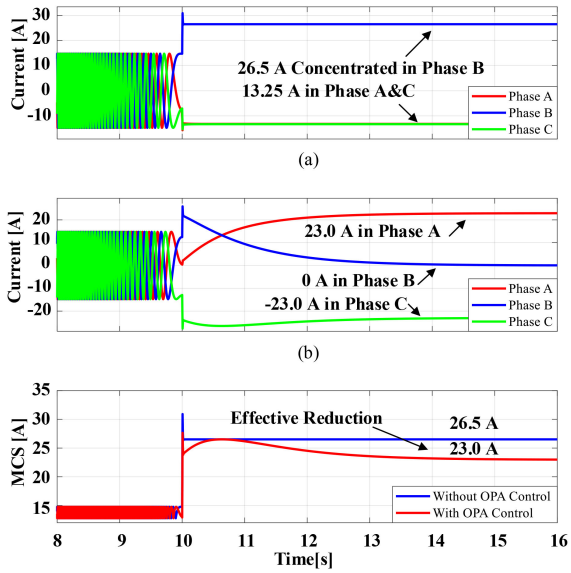

Fig. 3. Current stress with original control (without OPA control) and current stress with OPA control in simulation validation. (a) Current stress contribution in electric system without OPA. (b) Current stress contribution in electric system with OPA control.

will be focused on the stall condition and the transition from the deceleration to the stall condition.

The current stress on the power semiconductor devices is compared in Fig. 3. With OPA control, the maximum current stress is reduced from 26.5 to 23 A, within less than 4 s adjustment. In the simulation, as the thermal coupling effect of Phase B is designed the strongest, the current stress of Phase B is redistributed to the minimum. Correspondingly, the thermal stress on the power semiconductor devices is also compared in Fig. 4. The highest junction node temperature (upper IGBT chip in the electrical B phase and upper IGBT in the electrical A phase) is reduced from 77 °C to 68 °C (15%), with a 5.6 W power losses reduction. What is more, the performance of reduction is significantly influenced by the detailed operation capacity and device selection, which is not concerned in this letter.

The mechanical response of the drive system is compared in Fig. 5. During the transition from deceleration to the stall condition, the stall condition is predicted and the speed reference is preswitched by applying OPA control. The rotor keeps rotating at a rather slow speed (less than 0.5 rad/s) until it reaches the OPA. What is more, the electromagnetic torque response can

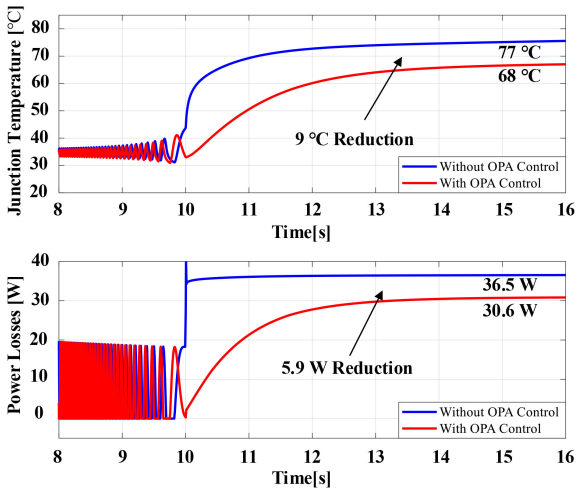

Fig. 4. Thermal stress with original control (without OPA control) and thermal stress with OPA control in simulation validation.

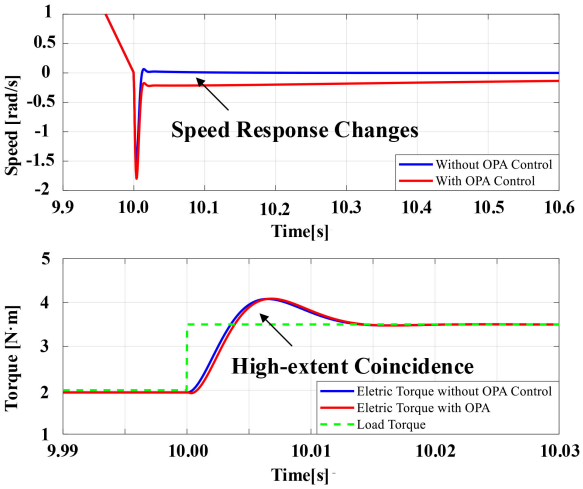

Fig. 5. Mechanical response with original control (without OPA control) and mechanical response with OPA control in simulation validation.

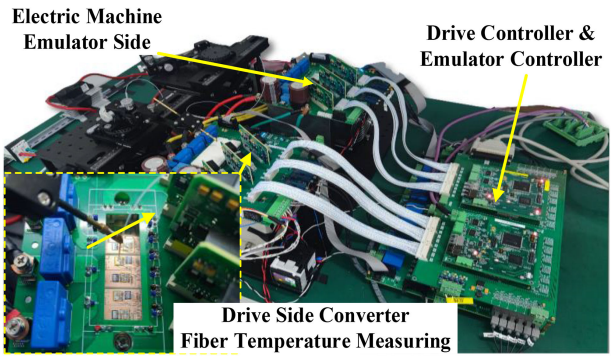

Fig. 6. Experiment setup.

still keep stable without any fluctuation. Compared with the one with original control, there is also a satisfying restoration of the dynamic performance.

The experimental setup is shown in Fig. 6. Instead of the electric machine drive system with actual PMSM, a full-bandwidth mission profile emulation of the electric machine system is

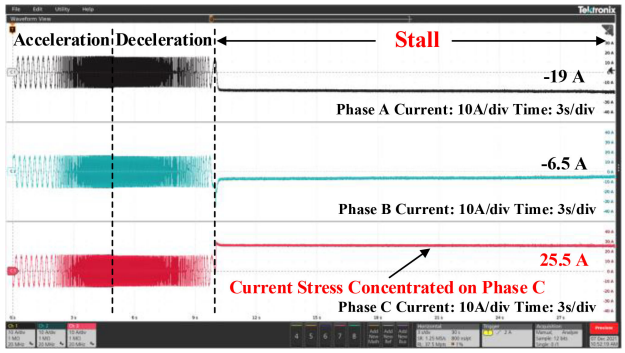

Fig. 7. Current stress with original FOC control (without OPA control) in experiment validation.

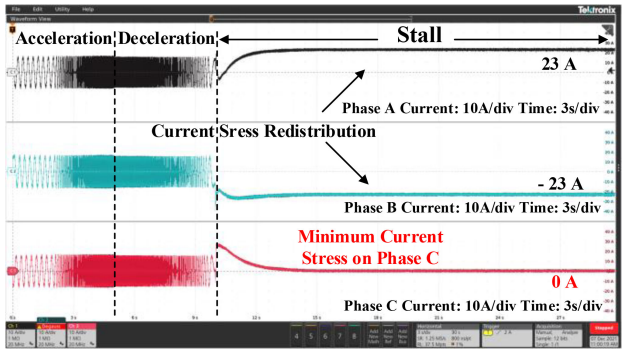

Fig. 8. Current stress with OPA control in experiment validation.

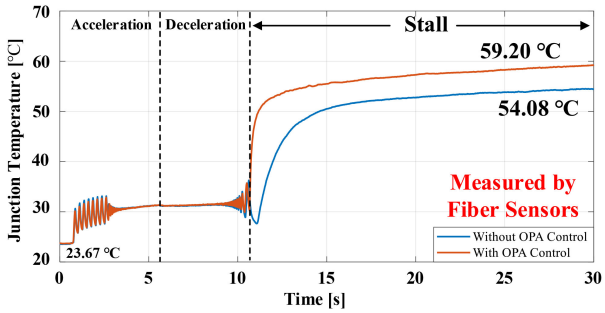

Fig. 9. Junction temperature response with original control and with OPA control in experiment validation (experimental measurement by fiber sensors).

adopted in this letter [13]. The drive controller and emulating controller are implemented on individual TMS320F28335 DSPs. The junction temperatures are measured directly by optical fiber temperature sensors. The parameters of the target emulating electric machine are listed in Table II [13], and the mission profile is set the same as the one in simulations.

To verify the robustness of the proposed OPA control method under specialized electrical and physical connection, the electrical connection mode of phase B and phase C is exchanged. Correspondingly, the θ_k should be set to phase C in (3), which suffers the strongest thermal coupling effect in the experiment.

The current stress is compared according to Figs. 7 and 8. By applying OPA control, the current stress behaviors during the common operation are not distorted, such as acceleration and deceleration. Moreover, the concentrated current stress on Phase C in the stall condition is well-redistributed to other phases, and

the maximum current stress of the whole drive inverter module is reduced from 25.5 to 23 A.

The junction temperatures response of the power semiconductor devices of the drive inverter is compared in Fig. 9, which suffers the maximum current stress (upper IGBT chip in the electrical C phase and upper IGBT in the electrical A phase). By applying OPA control, the thermal behavior is also not distorted during the common mission profile. Moreover, the highest junction temperature during the stall condition is also reduced from 59.20 °C to 54.08 °C (14.5%), which coincides with the result in the simulation well.

IV. Conclusion

An ATC method with OPA under stall condition of electric machine system is proposed in this letter. By applying an additional mechanical phase angle control loop, the electrical and mechanical phase angle is controlled during the stall condition for the best electrothermal stress distribution. During the normal operation, the proposed method will not distort the behaviors of the original drive control system. During the stall condition, mechanical stability can be guaranteed and the maximum electrothermal stress can also be reduced by around 15%. Simulations and experimental results are provided to validate the effectiveness of the proposed method.

References

[1] K. Ma, H. Wang, and F. Blaabjerg, "New approaches to reliability assessment: Using physics-of-failure for prediction and design in power electronics systems," *IEEE Power Electron. Mag.*, vol. 3, no. 4, pp. 28–41, Dec. 2016.

[2] P. Wikstrom, L. A. Terens, and H. Kobi, "Reliability availability and maintainability of high-power variable-speed drive systems," *IEEE Trans. Ind. Appl.*, vol. 36, no. 1, pp. 231–241, Jan./Feb. 2000.

[3] K. Ma, S. Xia, Y. Qi, X. Cai, Y. Song, and F. Blaabjerg, "Power-electronics-based mission profile emulation and test for electric machine drive system - Concepts, features, and challenges," *IEEE Trans. Power Electron.*, vol. 37, no. 7, pp. 8526–8542, Jul. 2022.

[4] K. Ma, J. Wang, X. Cai, and F. Blaabjerg, "AC grid emulations for advanced testing of grid-connected converters-An overview," *IEEE Trans. Power Electron.*, vol. 36, no. 2, pp. 1626–1645, Feb. 2021.

[5] M. Andresen, K. Ma, G. Buticchi, J. Falck, F. Blaabjerg, and M. Liserre, "Junction temperature control for more reliable power electronics," *IEEE Trans. Power Electron.*, vol. 33, no. 1, pp. 765–776, Jan. 2018.

[6] J. Lemmens, P. Vanassche, and J. Driesen, "Optimal control of traction motor drives under electrothermal constraints," *IEEE Trans. Emerg. Sel. Topics Power Electron.*, vol. 2, no. 2, pp. 249–263, Jun. 2014.

[7] T. A. Polom, B. Wang, and R. D. Lorenz, "Control of junction temperature and its rate of change at thermal boundaries via precise loss manipulation," *IEEE Trans. Ind. Appl.*, vol. 53, no. 5, pp. 4796–4806, Sep./Oct. 2017.

[8] C. H. V. D. Broeck and R. W. De Doncker, "Increasing torque capability of AC drives via active thermal management of inverters," *IEEE Trans. Ind. Appl.*, vol. 57, no. 6, pp. 6277–6287, Nov./Dec. 2021.

[9] *Standard Practices Cycle Counting Fatigue Analysis*, ASTM International, IEEE Standard E1049-85, 2005.

[10] Y. Ko, M. Andresen, G. Buticchi, and M. Liserre, "Discontinuous-modulation-based active thermal control of power electronic modules in wind farms," *IEEE Trans. Power Electron.*, vol. 34, no. 1, pp. 301–310, Jan. 2019.

[11] M. Karami, R. Tallam, and R. Cuzner, "Power cycling of three-level inverters for low speed operation," in *Proc. IEEE Appl. Power Electron. Conf. Expo.*, 2020, pp. 2492–2498.

[12] L. Wei, J. McGuire, and R. A. Lukaszewski, "Analysis of PWM frequency control to improve the lifetime of PWM inverter," *IEEE Trans. Ind. Appl.*, vol. 47, no. 2, pp. 922–929, Mar./Apr. 2011.

[13] S. Ali, S. Bhattacharya, D. Mascarella, and G. Joos, "Thermal management during stalled rotor by conduction loss redistribution," in *Proc. Transp. Electrific. Conf. Expo.*, 2015, pp. 1–6.

[14] A. S. Bahman, K. Ma, and F. Blaabjerg, "A lumped thermal model including thermal coupling and thermal boundary conditions for high power IGBT modules," *IEEE Trans. Power Electron.*, vol. 22, no. 3, pp. 2518–2530, 2018.

[15] P. C. Krause, O. Wasynczuk, and S. D. Sudhoff, *Analysis of Electric Machinery and Drive Systems*. Hoboken, NJ, USA: Wiley, 2002, pp. 191–206.

[16] Y. Qi, K. Ma, and W. Tang, "Full-bandwidth mission profile emulation of electric machine system with voltage reference signal transmission," *IEEE Trans. Power Electron.*, vol. 37, no. 3, pp. 3473–3483, Mar. 2022.